Supplemental information

PITPNC1 promotes the thermogenesis of brown adipose tissue under acute cold exposure

Guoqing Tang, Chengxin Ma, Liangkui Li, Shaoyan Zhang, Fengsheng Li, Jin Wu, Yesheng Yin, Qing Zhu, Yan Liang, Ru Wang, He Huang, Tong-Jin Zhao, Hongyuan Yang, Peng Li, and Feng-Jung Chen

Data Availability Statement:

The data that supports the findings of this study are available in the supplementary material of this article.

Supplementary Materials:

Figures S1 to S6; Table S1.

Figure S1

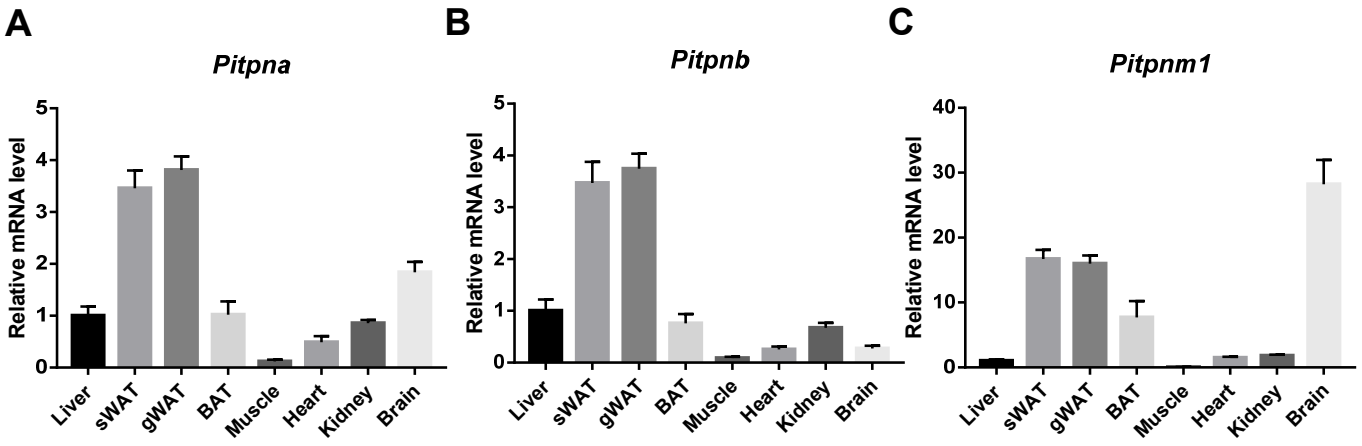
A
Pitpna
Relative mRNA level
0
1
2
3
4
5
Liver
sWAT
gWAT
BAT
Muscle
Heart
Kidney
Brain
B
Pitpnb
Relative mRNA level
0
1
2
3
4
5
Liver
sWAT
gWAT
BAT
Muscle
Heart
Kidney
Brain
C
Pitpnm1
Relative mRNA level
0
10
20
30
40
Liver
sWAT
gWAT
BAT
Muscle
Heart
Kidney
Brain

Figure S1. The transcriptional profile of PITP family proteins in wildtype mice. Related to Figure 1.

A-C, Relative mRNA levels of *Pitpna* (A), *Pitpnb* (B), and *Pitpnm1* (C) in various tissues of wildtype mice.

Figure S2

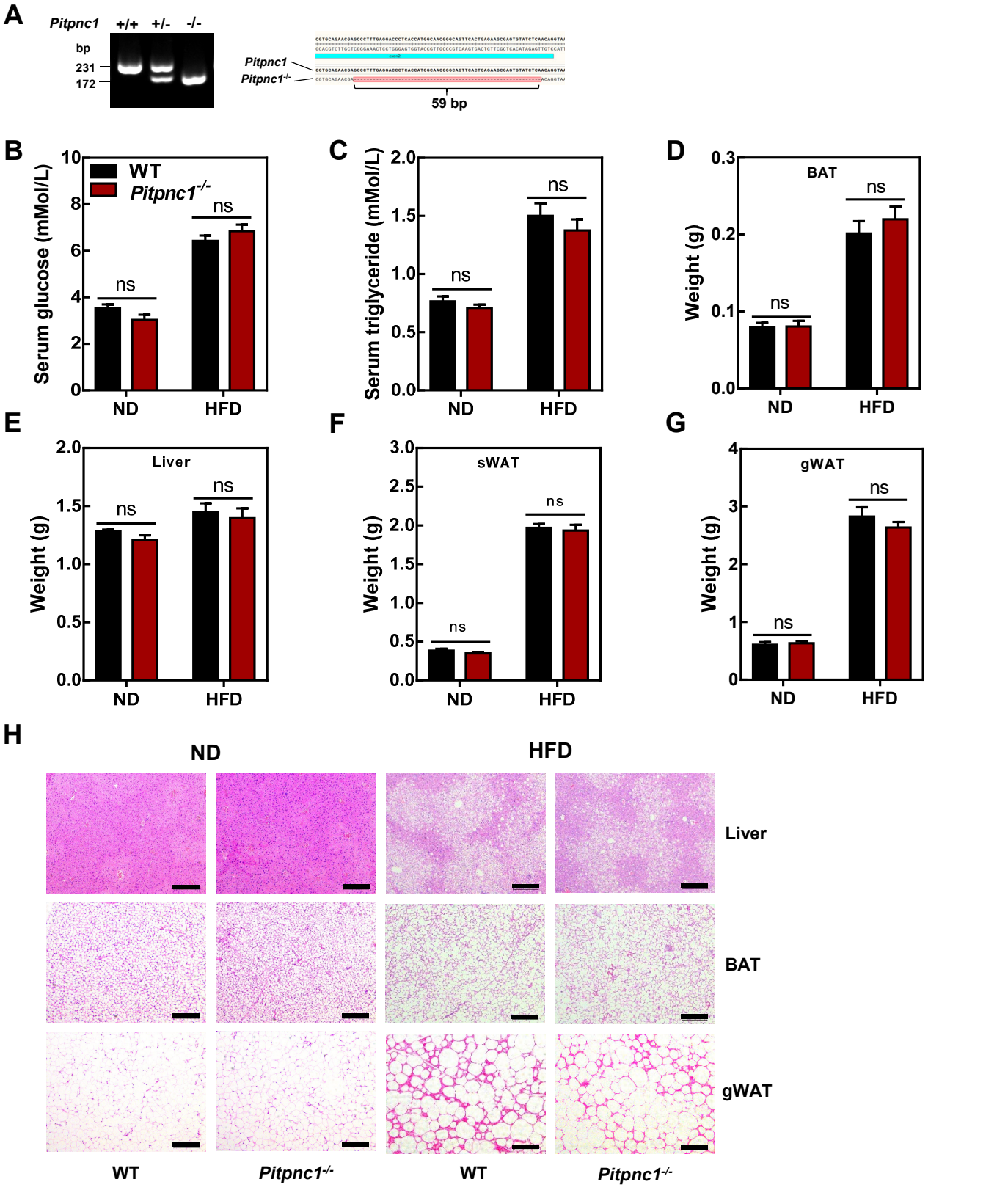
A
Pitpnc1 +/+ +/- -/-
bp
231
172
Pitpnc1
Pitpnc1-/-
59 bp
B
Serum glucose (mMol/L)
WT
Pitpnc1-/-
ns
ND
HFD
C
Serum triglyceride (mMol/L)
D
BAT
Weight (g)
E
Liver
F
sWAT
G
gWAT
H
ND
HFD
Liver
BAT
gWAT
WT
Pitpnc1-/-

Figure S2. The physiological properties of *Pitpnc1*$^{-/-}$ mice under various nutrient treatments. Related to Figure 2.

A, The results of sequencing were completed in accordance to our construction strategy.

B-G, Male littermates (6-week-old) of WT and *Pitpnc1*$^{-/-}$ mice were fed either normal chow diet (ND) or high-fat diet (HFD) for 16 weeks. At week 16, the levels of serum glucose (B) and serum triglyceride (C) and the weight of brown adipose tissue (BAT) (D), liver (E), subcutaneous adipose tissue (sWAT) (F), gonadal adipose tissue (gWAT) (G) in the two mouse strains were measured.

H, H&E images of liver, BAT, and gWAT extracted from the two mouse strains after the treatments of 16-weeks ND and HFD, respectively. Scale bars, 200 μm.

Mean ± SEM in (B)–(G). Two-tailed Student's t test in (B)–(G).

Figure S3

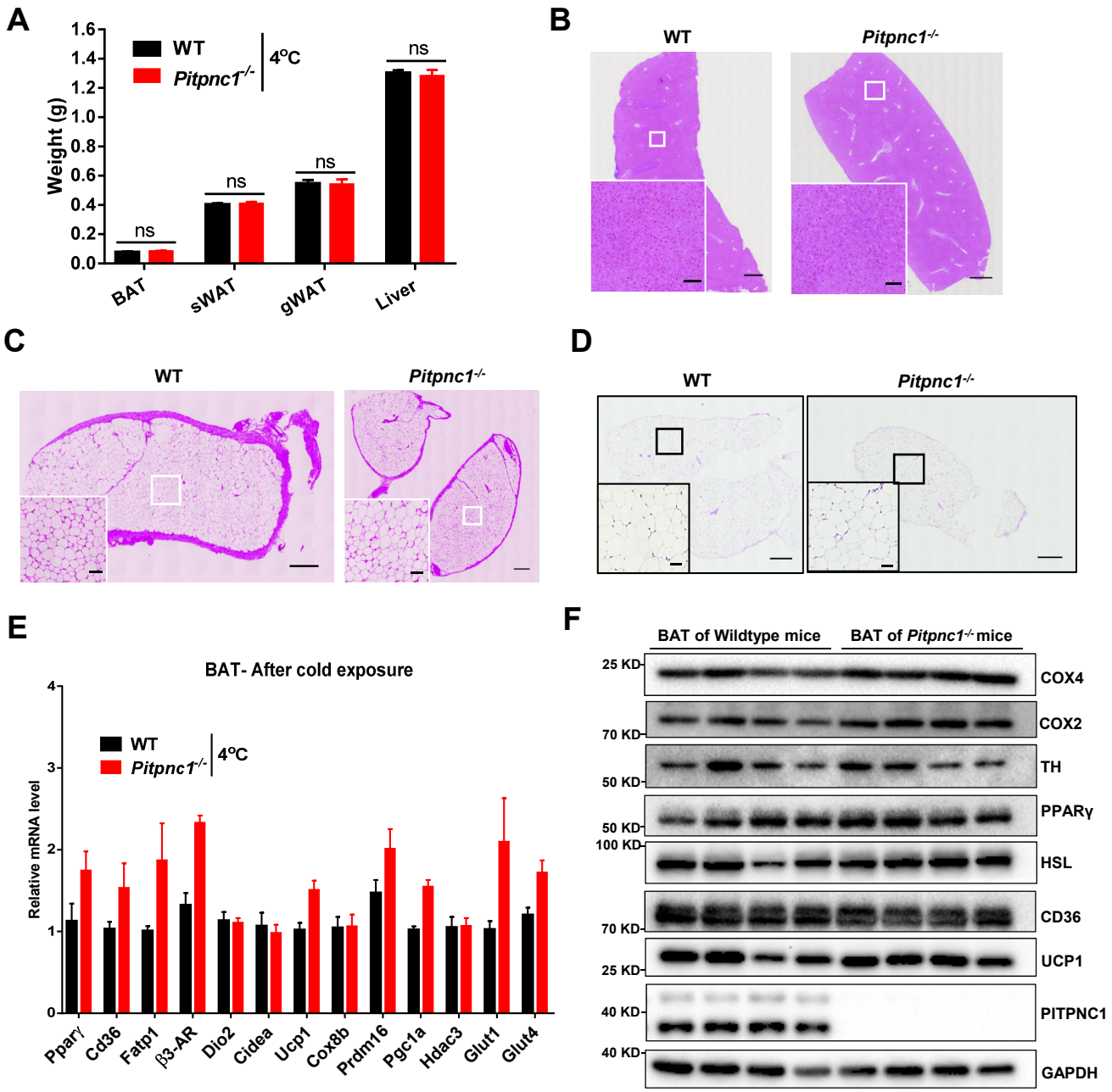
A
WT
Pitpnc1-/-
4°C
Weight (g)
1.6
1.4
1.2
1.0
0.8
0.6
0.4
0.2
0.0
ns
BAT
sWAT
gWAT
Liver
B
WT
Pitpnc1-/-
C
WT
Pitpnc1-/-
D
WT
Pitpnc1-/-
E
BAT- After cold exposure
WT
Pitpnc1-/-
4°C
Relative mRNA level
4
3
2
1
0
Pparγ
Cd36
Fatp1
β3-AR
Dio2
Cidea
Ucp1
Cox8b
Prdm16
Pgc1a
Hdac3
Glut1
Glut4
F
BAT of Wildtype mice
BAT of Pitpnc1-/- mice
25 KD
COX4
70 KD
COX2
50 KD
TH
50 KD
PPARγ
100 KD
HSL
70 KD
CD36
25 KD
UCP1
40 KD
PITPNC1
40 KD
GAPDH

Figure S3. The physiological properties of *Pitpnc1*$^{-/-}$ mice after acute cold exposure. Related to Figure 3.

A, Single-housed 8-week-old male littermates of wildtype mice and *Pitpnc1*$^{-/-}$ mice were fasted for 4 h and then switched to 4°C for 4 h. At the end of the experiment, the mice were dissected. The weight of brown adipose tissue (BAT), subcutaneous adipose tissue (sWAT), gonadal adipose tissue (gWAT), or liver in the two mouse strains was measured. Each value represents mean ± SEM from 5 mice.

B-D, Representative H&E images show the change in lipid content in the liver (B), sWAT (C), and gWAT (D) between the two mouse strains in (A).

E-F, The relative mRNA levels of indicated genes (E) and the expression levels of indicated proteins (F) in the BAT of the two mouse strains under acute cold exposure were measured. Four mice were used in each group.

Mean ± SEM in (A) and (E). Two-tailed Student's t test in (A) and (E). Scale bars, 300 μm in (B)-(D); (Enlarge) 50 μm in (B)-(D).

Figure S4

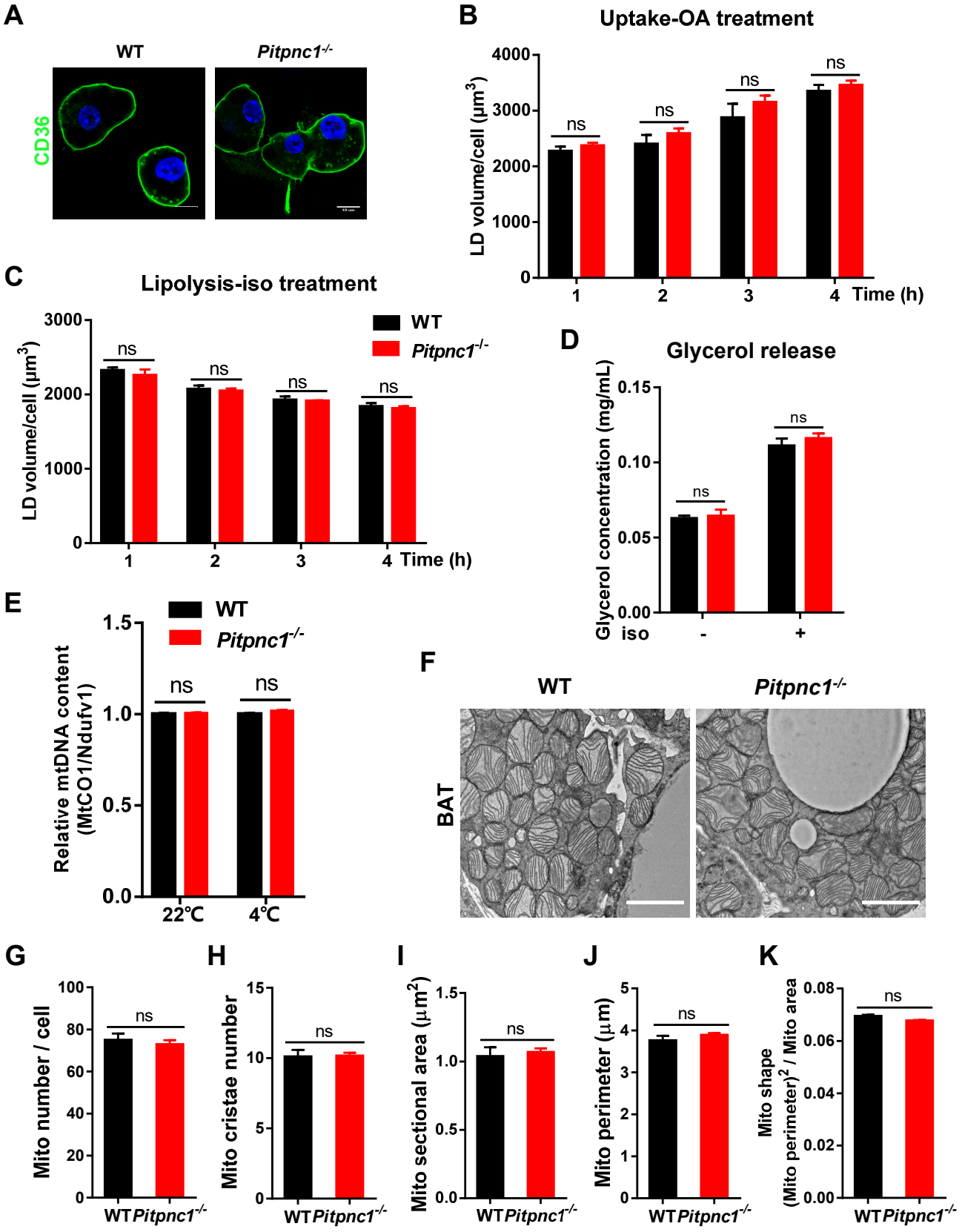
A
WT
Pitpnc1-/-
CD36
B
Uptake-OA treatment
LD volume/cell (μm3)
4000
3000
2000
1000
0
ns
1
2
3
4 Time (h)
C
Lipolysis-iso treatment
WT
Pitpnc1-/-
LD volume/cell (μm3)
3000
2000
1000
0
ns
1
2
3
4 Time (h)
D
Glycerol release
Glycerol concentration (mg/mL)
0.15
0.10
0.05
0.00
ns
iso
-
+
E
WT
Pitpnc1-/-
Relative mtDNA content (MtCO1/Ndufv1)
1.5
1.0
0.5
0.0
ns
22℃
4℃
F
WT
Pitpnc1-/-
BAT
G
Mito number / cell
100
80
60
40
20
0
ns
WT
Pitpnc1-/-
H
Mito cristae number
15
10
5
0
ns
WT
Pitpnc1-/-
I
Mito sectional area (μm2)
1.5
1.0
0.5
0.0
ns
WT
Pitpnc1-/-
J
Mito perimeter (μm)
5
4
3
2
1
0
ns
WT
Pitpnc1-/-
K
Mito shape (Mito perimeter)2 / Mito area
0.08
0.06
0.04
0.02
0.00
ns
WT
Pitpnc1-/-

Figure S4. Properties of mitochondria from the BAT of wildtype mice and *Pitpnc1*$^{-/-}$ mice. Related to Figure 4.

A-D, Mature brown adipocytes were differentiated from the BAT-SVF cells of wildtype mice and *Pitpnc1*$^{-/-}$ mice. Images show the localization of endogenous CD36 at plasma membrane of 7-days mature brown adipocytes (A). Scale bar, 10 μm. The total lipid droplet (LD) volume in every mature brown adipocyte after treatment of 200 μM oleic acids was measured (B). The total LD volume in every mature brown adipocyte (C) and the glycerol level in medium released from the mature brown adipocytes (D) after isoproterenol treatment were measured for lipolysis evaluation.

E, Relative mitochondrial (mt) DNA content in BAT was assessed by qPCR and calculated from copy number of the mtDNA encoded *MtCO1* gene and the nuclear DNA encoded *Ndufv1* gene of mitochondria in the BAT of the two mouse strains at 22°C or 4°C (n = 6 cells).

F, Representative electron microscopy images show the morphology of mitochondria in the BAT of the two mouse strains. Scale bars, 2 μm.

G-K, The morphological features of mitochondria in (F) were quantified by five parameters: mitochondria number per cell (n = 26 cells) (G), mitochondrial cristae number (H), sectional area of a mitochondrion (I), perimeter of a mitochondrion (J), and mitochondrial shape using the simple ratio of S^2/A (K) (n > 100 mitochondria) as described in Methods.

Mean ± SEM in (B)-(E) and (G)-(K). Two-tailed Student's t test in (B)-(E) and (G)-(K).

Figure S5

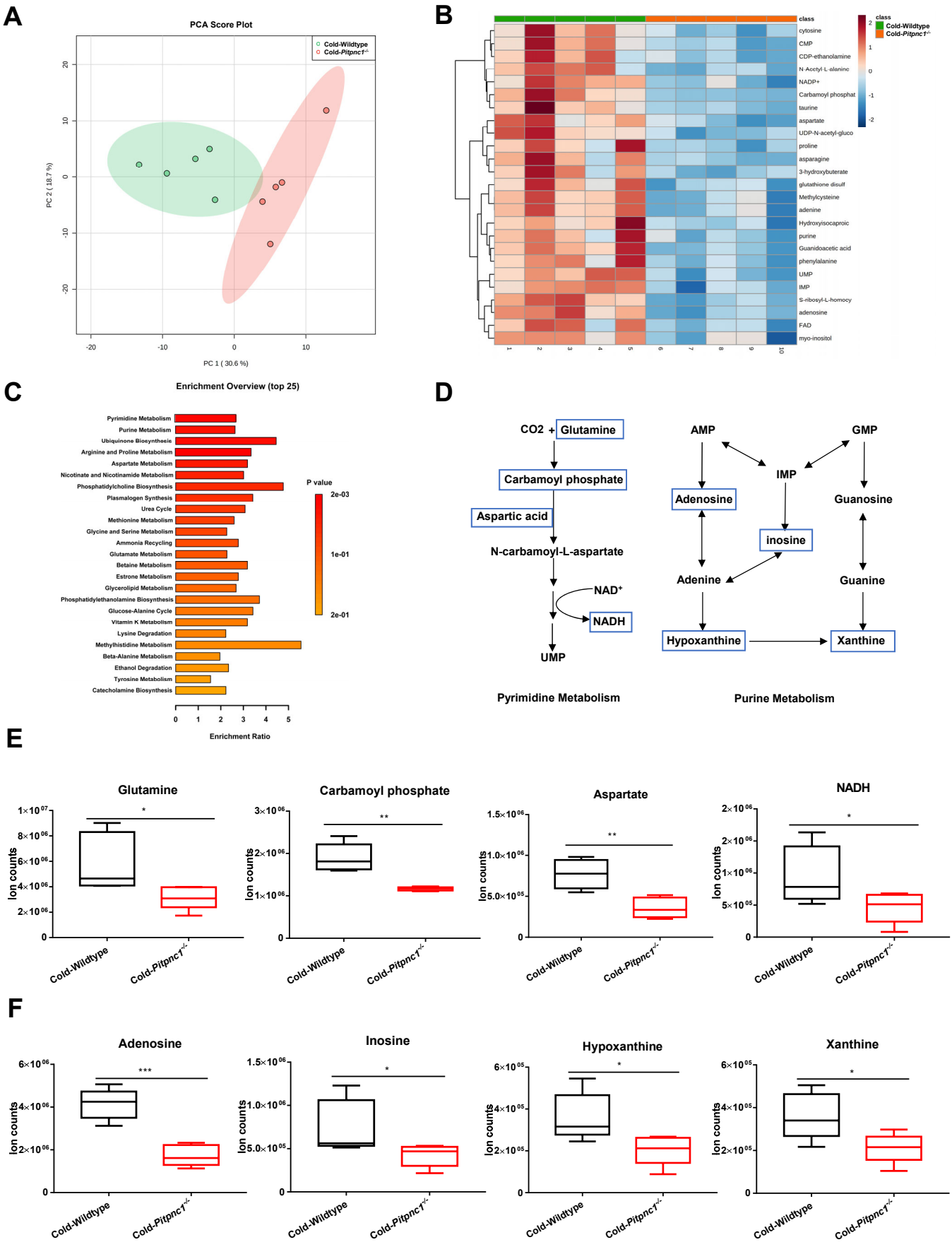
A
PCA Score Plot
Cold-Wildtype
Cold-Pitpnc1-/-
PC 2 (18.7 %)
PC 1 (30.6 %)
B
class
Cold-Wildtype
Cold-Pitpnc1-/-
cytosine
CMP
CDP-ethanolamine
N-Acetyl-L-alaninc
NADP+
Carbamoyl phosphat
taurine
aspartate
UDP-N-acetyl-gluco
proline
asparagine
3-hydroxybuterate
glutathione disulf
Methylcysteine
adenine
Hydroxyisocaproic
purine
Guanidoacetic acid
phenylalanine
UMP
IMP
S-ribosyl-L-homocy
adenosine
FAD
myo-inositol
C
Enrichment Overview (top 25)
Pyrimidine Metabolism
Purine Metabolism
Ubiquinone Biosynthesis
Arginine and Proline Metabolism
Aspartate Metabolism
Nicotinate and Nicotinamide Metabolism
Phosphatidylcholine Biosynthesis
Plasmalogen Synthesis
Urea Cycle
Methionine Metabolism
Glycine and Serine Metabolism
Ammonia Recycling
Glutamate Metabolism
Betaine Metabolism
Estrone Metabolism
Glycerolipid Metabolism
Phosphatidylethanolamine Biosynthesis
Glucose-Alanine Cycle
Vitamin K Metabolism
Lysine Degradation
Methylhistidine Metabolism
Beta-Alanine Metabolism
Ethanol Degradation
Tyrosine Metabolism
Catecholamine Biosynthesis
P value
2e-03
1e-01
2e-01
Enrichment Ratio
D
CO2 + Glutamine
Carbamoyl phosphate
Aspartic acid
N-carbamoyl-L-aspartate
NAD+
NADH
UMP
Pyrimidine Metabolism
AMP
GMP
IMP
Adenosine
Guanosine
inosine
Adenine
Guanine
Hypoxanthine
Xanthine
Purine Metabolism
E
Glutamine
Carbamoyl phosphate
Aspartate
NADH
Ion counts
Cold-Wildtype
Cold-Pitpnc1-/-
F
Adenosine
Inosine
Hypoxanthine
Xanthine
Ion counts
Cold-Wildtype
Cold-Pitpnc1-/-

Figure S5. Metabolomics shows deficient thermogenesis-associated pathways in the BAT of *Pitpnc1*$^{-/-}$ mice. Related to Figure 5.

A and B,

Single-housed 8-week-old male littermates of wildtype mice and *Pitpnc1*$^{-/-}$ mice were fasted for 4 h and then switched to 4°C for 4 h. At the end of the experiment, the mice were dissected and BATs were collected for metabolomics. PCA score plot (A) and hierarchical clustered heatmaps (B) of two metabolic datasets derived from the purified mitochondria in the BAT of the two mouse strains were calculated and summarized. The hierarchical clustered heatmaps shows top 25 metabolite variations.

C, KEGG metabolic pathways enrichment analysis for the two metabolic datasets in (A).

D, Schematic diagram shows pyrimidine metabolism (left) and purine metabolism (right) pathways.

E and F,

Variation analysis of metabolites in a pyrimidine metabolism pathway (E) or in a purine metabolism pathway (F) was derived from (B).

Mean ± SEM in (E) and (F). Two-tailed Student's t test in (E) and (F).

Figure S6

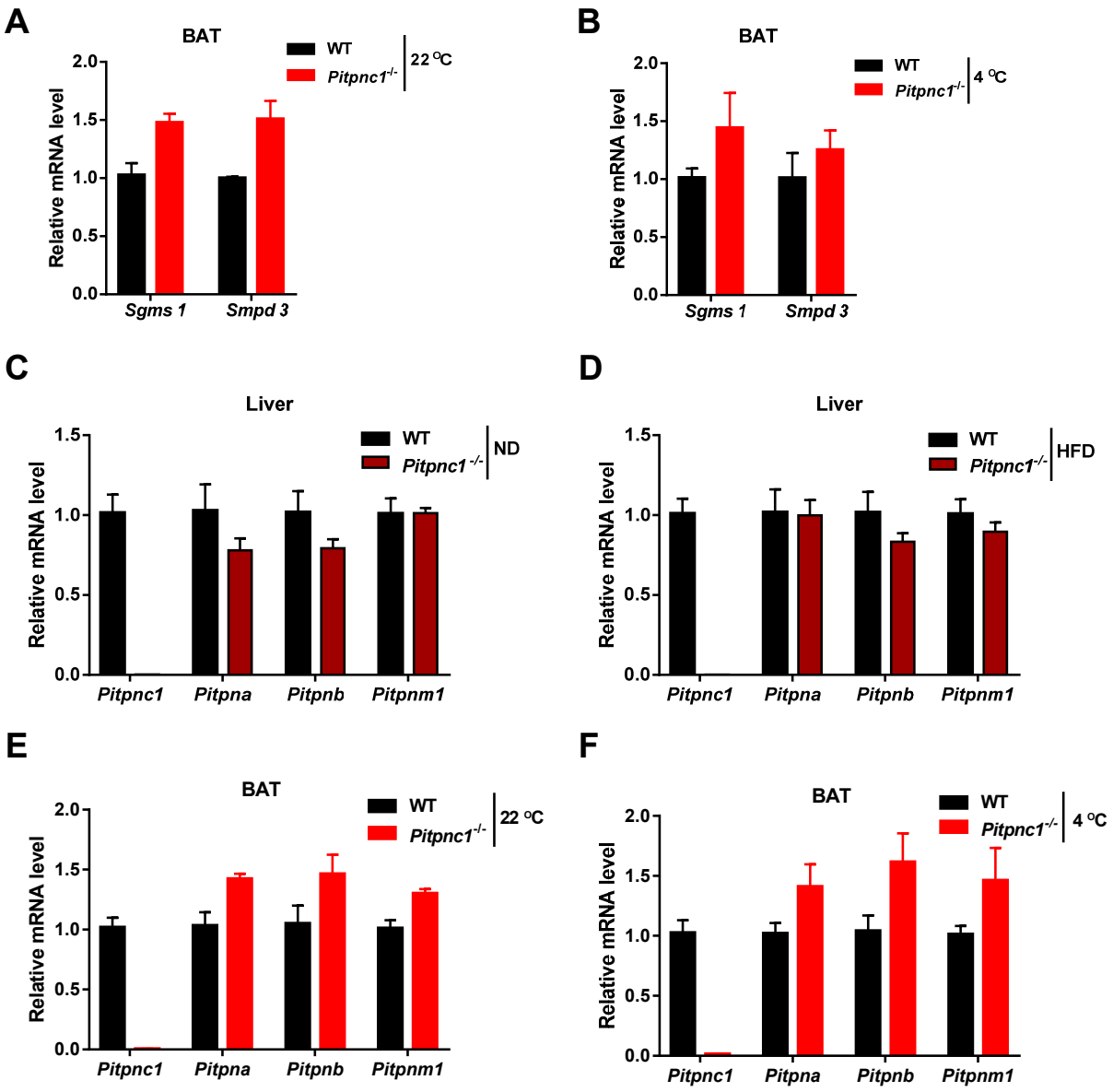
A
BAT
WT
Pitpnc1-/-
22 ℃
Relative mRNA level
2.0
1.5
1.0
0.5
0.0
Sgms 1
Smpd 3
B
BAT
WT
Pitpnc1-/-
4 ℃
Relative mRNA level
Sgms 1
Smpd 3
C
Liver
WT
Pitpnc1 -/-
ND
Relative mRNA level
1.5
1.0
0.5
0.0
Pitpnc1
Pitpna
Pitpnb
Pitpnm1
D
Liver
WT
Pitpnc1-/-
HFD
Relative mRNA level
Pitpnc1
Pitpna
Pitpnb
Pitpnm1
E
BAT
WT
Pitpnc1-/-
22 ℃
Relative mRNA level
2.0
1.5
1.0
0.5
0.0
Pitpnc1
Pitpna
Pitpnb
Pitpnm1
F
BAT
WT
Pitpnc1-/-
4 ℃
Relative mRNA level
Pitpnc1
Pitpna
Pitpnb
Pitpnm1

Figure S6. The transcriptional profile of key enzymes for lipid conversion and PITP family proteins. Related to Figure 5.

A and B,

Relative mRNA levels of indicated enzymes for lipid conversion from PC to ceramide in the BAT of wildtype mice and *Pitpnc1*$^{-/-}$ mice at room temperature (A) or under acute cold exposure (B). Six mice were used in each group.

C-F, Relative mRNA levels of *Pitpna*, *Pitpnb*, and *Pitpnm1* in the liver of the two mouse strains after the treatments of 16-weeks normal chow diet (ND) (C) or high-fat diet (HFD) (D) or in the BAT of the two mouse strains at room temperature (E) or after acute cold exposure (F). Three mice (for diet treatment) or six mice (for cold challenge) were used in each group.

Mean ± SEM in (A)-(F). Two-tailed Student's t test in (A)-(F).

Table S1. List of the primers used in this study.

Gene name	Primer sequence
Dio2-mus-F	GTCCGCAAATGACCCCTTT
Dio2-mus-R	CCCACCCACTCTCTGACTTTC
Fatp1-mus-F	CCGTATCCTCACGCATGTGT
Fatp1-mus-R	CTCCATCGTGTCCTCAATGAC
Glut1-mus-F	GGTGTGCAGCAGCCTGTGTA
Glut1-mus-R	CAACAAACAGCGACACCACAGT
Glut4-mus-F	CCGGCAGCCTCTGATCAT
Glut4-mus-R	CCGACTCGAAGATGCTGGTT
Pgc1a-mus-F	GACTCAGTGTCACCACCGAAA
Pgc1a-mus-R	TGAACGAGAGCGCATCCTT
Prdm16-mus-F	CAGCACGGTGAAGCCATTC
Prdm16-mus-R	GCGTGCATTCGCTTGTG
Pparγ-mus-F	GCCCTTTGGTGACTTTATGGA
Pparγ-mus-R	GCAGCAGGTTGTCTTGGATG
Ucp1-mus-F	AAGCTGTGCGATGTCCATGT
Ucp1-mus-R	AAGCCACAAACCCTTTGAAAA
β3-AR-mus-F	TCCTTCTACCTTCCCCTCCTT
β3-AR-mus-R	CGGCTTAGCCACAACGAACAC
Hdac3-mus-F	CACCAAGAGCCTTGATGCCTT
Hdac3-mus-R	GCAGCTCCAGGATACCAATTACT
Cidea-mus-F	TGACATTCATGGGATTGCAGAC
Cidea-mus-R	GGCCAGTTGTGATGACTAAGAC
Cox8b-mus-F	TGTGGGGATCTCAGCCATAGT
Cox8b-mus-R	AGTGGGCTAAGACCCATCCTG
Cd36-mus-F	ATGGGCTGTGATCGGAACTG
Cd36-mus-R	GTCTTCCCAATAAGCATGTCTCC